DOI:10.11835/j.issn.2096-6717.2020.088 开放科学(资源服务)标识码(OSID):

Adsorption of sulfate ions on zirconium-loaded granular activated carbon in aqueous solution

HONG Yixia, *CAO Wei*, *AO Hanting*, *XING Xiaolei*, *LI Xin*

(College of Civil Engineering, Huaqiao University, Xiamen 361021, Fujian, P. R. China)

Abstract: Zirconium oxide-loaded granular activated carbon (Zr-GAC) was prepared for the adsorption of sulfate ions in aqueous solution. The Zr-GAC was characterized by scanning electron microscopy (SEM), X-ray diffraction (XRD), X-ray photoelecton spectroscopy (XPS), and specific surface area measurement. The results showed that the Zr-GAC had a porous surface with many aggregates, composed of zirconium oxides. XPS analysis confirmed the massive presence of zirconium and hydroxyl groups in the adsorbent surface. The specific surface area of the activated carbon decreased after modification with zirconium oxides. Batch adsorption experiments were conducted to determine the effect of pH on sulfate adsorption, and it was found that better adsorption could be achieved at pH lower than 10. Modeling analysis of the adsorption isotherms showed that the Dubinin-Radushkevich (D-R) equation had better fittings than the Langmuir model, and the maximum adsorption capacity of the Zr-GAC determined by the D-R equation was 70.14 mg/g in neutral water solution, much higher than that of raw GAC (8.9 mg/g). The D-R equation may have a problem in determining the adsorption energy for a solution adsorption, which deserves more research. Kinetic studies show that the adsorption of sulfate on the Zr-GAC is relatively fast, and it follows the pseudo second-order kinetic equation. In addition, an increase of temperature may facilitate the sulfate adsorption, to some extent. The Zr-GAC showed good potential for the adsorption of sulfate ions in aqueous solution. It exhibited approximately twice the adsorption capacity and a much wider applicable range of pH compared with the zirconium-loaded biochar adsorbent.

Keywords: sulfate ion; adsorption; granular activated carbon; zirconium oxides; Dubinin-Radushkevich equation

载锆颗粒活性炭吸附去除水溶液中的硫酸根离子

洪怡霞,曹威,敖涵婷,邢小蕾,李欣

(华侨大学 土木工程学院,福建 厦门 361021)

摘 要:制备负载氧化锆的颗粒活性炭(Zr-GAC),以吸附水溶液中的硫酸根离子。采用扫描电镜(SEM)、X 射线衍射(XRD)、X 射线光电子能谱(XPS)和比表面积测定等方法对 Zr-GAC 进行表

Received:2020-05-26

Foundation items: National Natural Science Foundation of China (No. 51408239); Natural Science Foundation of Fujian Province (No. 2016J01193); the Fundamental Research Funds for the Central Universities (No. ZQN-712); Subsidized Project for Postgraduates' Innovative Fund in Scientific Research of Huaqiao University.

Author brief: HONG Yixia (1995-), main research interest: wastewater treatment and utilization, E-mail: 1648556595@qq.com.

CAO Wei (corresponding author), PhD, associate professor, E-mail: weicao@hqu.edu.cn.

征。结果表明,Zr-GAC 具有多孔的表面积,其上具有许多由氧化锆组成的团聚体。XPS 分析证实,吸附剂表面存在大量的锆和羟基,氧化锆改性后的活性炭比表面积减小。采用间歇吸附实验研究了 pH 值对硫酸盐吸附的影响,在 pH 值小于 10 时,吸附效果较好。吸附等温线的模拟分析表明,Dubinin-Radushkevich(D-R)方程比 Langmuir 模型具有更好的拟合性,由 D-R 方程确定的在中性水溶液最大吸附量为 70.14 mg/g,远高于原 GAC(8.9 mg/g)。需要注意的是,D-R 方程在测定溶液吸附的吸附能时可能存在问题,值得进一步研究。动力学研究表明,硫酸根在 Zr-GAC 上的吸附速度较快,并遵循准二级动力学方程。此外,温度的升高在一定程度上可能利于硫酸盐的吸附。Zr-GAC 具有很好的吸附水溶液中硫酸根离子的潜力,特别是其吸附容量约为载锆生物炭吸附剂的两倍,pH 值的适用范围更广。

关键词:硫酸根;吸附;颗粒活性炭;氧化锆;Dubinin-Radushkevich 方程

中图分类号:X703.5 **文献标志码**:A **文章编号**:2096-6717(2021)01-0203-12

1 Introduction

Sulfate ions exist widely in surface water, groundwater, and industrial wastewater. The main sources of sulfate ions in natural water are chemical weathering and oxidation processes of sulfur-containing minerals. Although sulfate ions are often thought to be non-toxic, their harm to the human body and the environment cannot be ignored. Excess ingestion of water containing sulfate ions for several months can cause obvious physiological damage to mammals[1]. High concentration of sulfate ions could threaten the safety of drinking water. According to the Standards for Drinking Water Quality of China, and also recommended by the WHO, the USA, and Japan, the concentration limit in drinking water of sulfate ions is 250 mg/L. Therefore, sulfate ions need to be removed from polluted water, which can be accomplished by freezing, purging, chemical precipitation (barium or calcium ion addition), membrane filtration, adsorption, ion exchange and biological treatment (sulfate-reducing bacteria)[2-5]. Adsorption separation is widely used because of its rapid and effective removal of sulfate ions. The adsorbent plays an important role in determining the effectiveness of the adsorption technology. The chosen adsorbent needs to have low cost, high adsorption capacity, and be renewable. In recent years, many adsorbents for removing sulfate ions, both inorganic and organic, have been reported. High-phosphorus iron ore waste is used as a new green adsorbent to purify and remove sulfate in groundwater[6], The sulfate absorption characteristics of the granular chitosan adsorbent in aqueous solution were studied in a fixed-bed column system[7]. Among many adsorbents, activated carbon is the one most intensively used in the treatment of drinking water. However, both granular and particle activated carbon exhibit a poor adsorption capacity for negatively charged sulfate ions.

Tetravalent zirconium was found to have a chemical affinity with sulfate ions, and zirconium hydroxide has been applied to control the sulfate ion content in brine feed of the chlor-alkali plant[8-9]. Recent studies have reported that coating zirconium oxides on solid substrate improves the adsorption of sulfate ions from water. Mulinari and Silva[10] prepared a sugarcane bagasse/zirconium oxide hybrid material for removing sulfate ions from wastewater. In a recent study, a zirconium-loaded biochar adsorbent was prepared to remove sulfate ions from water[11]. However, its capacity to adsorb sulfate ions was approximately 40 mg/g, which is not satisfactory. Activated carbon perhaps is more suitable as a support material because of its porous structure, high specific surface area, chemical stability, and hygienic conditions. Zirconium-loaded activated carbon has been proposed for the removal of

arsenic[12], fluoride[13] and phosphate[14] from wastewater. However, literature investigation shows that there are few reports on the application of zirconium-modified activated carbon for the adsorption of sulfate ions. The enhancement effect of zirconium-modification on the adsorption of sulfate by activated carbon and zirconium-loaded activated carbon is not clear. More research on this is needed.

In this work, zirconium oxides are loaded onto the surface of granular activated carbon (GAC) in a simple way that is chemical precipitation with zirconium oxychloride in ammonia water. The prepared zirconium oxide-loaded granular activated carbon (Zr-GAC) is characterized with scanning electron microscopy (SEM), X-ray photoelectron spectrum (XPS), and X-ray diffraction (XRD) and specific surface area measurement. The adsorption equilibrium and kinetics of the sulfate ions on Zr-GAC are studied with batch adsorption experiments, and the results are discussed with adsorption isotherm models, including the Langmuir model, the Dubinin-Radushkevich (D-R) equation, and adsorption kinetic equations.

2 Materials and methods

2.1 Materials and chemicals

The GAC with a particle size ranging from 0.1 to 1.5 mm was purchased from Sinopharm Chemical Reagent Co., Ltd., China. Chemicals such as zirconium oxychloride ($ZrOCl_2 \cdot 8H_2O$), ammonium solution ($NH_3 \cdot H_2O$), sodium sulfate (Na_2SO_4), sodium hydroxide (NaOH) and hydrochloric acid (HCl) were also bought from Sinopharm Chemical Reagent Co., Ltd., China. The stock solution of sulfate ions was prepared by dissolving dried sodium sulfate in deionized water. Solutions with required concentrations of sulfate ions were diluted from the stock solution in the adsorption experiments. Solution pH was adjusted with 0.1 mol/L NaOH and 0.1 mol/L HCl solution when there was a need. All chemicals were of analytical grade.

2.2 Preparation of zirconium oxide-loaded granular activated carbon

Zirconium was loaded on activated carbon by a simple method. First, four grams of zirconium oxychloride was dissolved in 100 mL 0.05 mol/L HCl solution, and five grams of GAC was immersed into this solution while stirring for 3 h. Second, the ammonium solution (1∶1) was added dropwise to the solution until solution pH reach 5.0. The mixed solution was stirred for 4 h. Third, solid material was separated from the solution by filtration, and washed with deionized water several times until the filtrate showed a neutral pH. Finally, the solid product was dried for 24 hours in an oven to obtain the Zr-GAC adsorbent.

2.3 Characterization of adsorbents

The surface morphology of GAC and Zr-GAC was probed by using SEM (S4800, Hitachi, Japan). The SEM images were obtained at an accelerating voltage varying from 5 to 20 kV. Surface groups of Zr-GAC were characterized by XPS (Escalab 250Xi, Thermo Fisher Scientific, USA). The monochromatized X-ray source was an Al K-alpha radiation (anode target). The XPS spectra were analyzed with XPS Peak 4.0 software. XRD patterns of the adsorbents were acquired with a Rigaku Ultima IV X-ray diffractometer (Rigaku, Japan) operated at 40 kV and 30 mA with Cu K-alpha radiation. The XRD patterns were recorded at a scanning speed of 5° per minute over the 2θ range from 10° to 90°. The data were analyzed with MDI Jade 5.0 software. The BET specific surface area of the materials was measured by N_2 adsorption/desorption isotherms at 77 K using a NOVA 2000e surface area analyzer (Quantachrome, USA).

2.4 Batch adsorption experiments

Batch adsorption experiments were carried out to measure the sulfate adsorption performance of Zr-GAC. 0.1 g of adsorbent was added to a 100 mL conical flask containing 50 mL sulfate ion solution.

The flask was placed in a shaker at 150 rpm and 298 K. After remaining in contact for 24 h, the solid adsorbent and the solution were separated by filtration, and the filtrate was collected to detect the sulfate concentration. The sulfate concentrations in the aqueous solution were measured using ion chromatography (Metrohm, Switzerland). The sulfate adsorption amount was calculated from Eq. (1).

$$q_e = \frac{C_0 - C_e \cdot V}{m} \quad (1)$$

where, C_0 and C_e (mg/L) are the initial and equilibrium sulfate concentration, respectively; V (L) is the volume of the sulfate ion solution; and m (g) is the mass of the adsorbent.

The effect of pH on the sulfate adsorption was investigated by varying the pH of the initial solution from 2.0 to 11.0. The variations of the sulfate adsorption amount with solution pH were measured at high and low initial sulfate concentration. Sulfate adsorption isotherms of GAC and Zr-GAC were determined by changing the sulfate concentration from 50 to 500 mg/L at a fixed adsorbent dose. Adsorption kinetic experiments were carried out with contact time intervals of 1, 2, 5, 10, 20, 30, 40, 50, and 60 min. All adsorption experimental samples were designed in duplicate.

3 Results and discussion

3.1 SEM images

SEM images of GAC and Zr-GAC are presented in Fig. 1. As shown in Fig. 1(a), smooth ridges and rough porous surfaces are observed over different sides of a GAC particle. There are long pare canals, cracks and attached fine particle on GAC surface, forming a complicated pore structure system. From the 1 000× magnification SEM image of GAC (Fig. 1(b)), it can be seen that many pores have a size ranging from several microns to approximately 30 um, which can be categorized as macropore according to earlier studies[15-16]. Fig. 1(c) shows that Zr-GAC surface is coated by a thin layer of unknown matter, which is believed to result from the zirconium-modification process. In the large magnification image (Fig. 1(d)), the thin layer is found to be small aggregates distributed unevenly on the surface of the activated carbon. The diameters of the aggregates vary from 0.5 to several microns. The qualitative analysis of the layer of aggregates on the activated carbon surface was performed by analyzing XRD patterns.

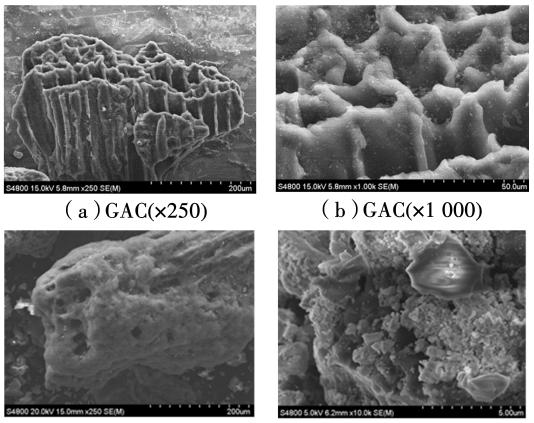

(a) GAC(×250) (b) GAC(×1 000)

(c) Zr-GAC(×250) (d) Zr-GAC(×1 000)

Fig. 1 Scanning electronic micrographs of GAC and Zr-GAC

3.2 XRD patterns

XRD patterns of GAC and Zr-GAC are shown in Fig. 2. For GAC, the diffraction profile exhibits broad peaks at the 2θ degree angle of 25° and 42°, which is attributed to the reflection from the (002) and (10) lattice planes of the graphite-like structure. This is in good agreement with previous studies on activated carbon[17-18]. The absence of a sharp diffraction peak suggests most GAC are in the form of amorphous carbon. The crystallinity of GAC is approximately 3%, determined by MDI Jade 5.0 software. The XRD pattern of Zr-GAC also the pattern of Zr-GAC at 2θ degree angles of 26°, 31°, 50°, and 58°, which are assigned to the (011), (111), (022) and (202) planes of the zirconia, respectively[19-21]. Therefore, XRD analysis can confirm the presence of zirconium oxides on the surface of Zr-GAC.

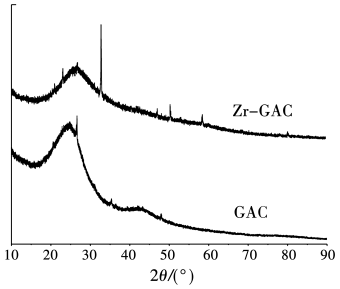

Fig. 2 X-ray diffraction patterns of GAC and Zr-GAC

3.3 XPS analysis

XPS characterizations of GAC and Zr-GAC were conducted to analyze the surface element composition and the functional groups. The element composition (atom %) of GAC and Zr-GAC from XPS full-spectra survey are presented in Table 1. The carbon atom content in GAC is more than 80%, and the O element accounts for approximately 11%, which should be from the O-containing groups on the surface of the activated carbon. A small quantity of N element in GAC may be related to the original material for activated carbon production. The carbon content in Zr-GAC decreases significantly in comparison with the loading of zirconium oxides. In addition, the appearance of chlorine in Zr-GAC results from the application of zirconium oxychloride during the preparation process.

Table 1 Element composition (atom %) on adsorbent surface from XPS full-spectra survey*

Adsorbents	C1s	O1s	N1s	Cl2p	Zr3d
GAC	83.67	11.61	1.52		
Zr-GAC	51.50	31.95	1.14	6.46	8.62

* The element with content less than 0.5% is not presented.

XPS analysis of C1s, O1s, and $Zr3d_{3/2}$ orbital for GAC and Zr-GAC is shown in Fig. 3. The C1s spectra are fitted to three components including the most intense peak at the binding energy of 284.8 eV, the peak around 286 eV, and the relatively weak band from 288.5 to 288.9 eV[22-23], as shown in Fig. 3(a). The peak at 284.8 eV is related to C—C/C—H bonds. The band from 288.5 to 288.9 eV is assigned to C=O and O—C—O linkages. The band around 286 eV is usually attributed to C—O bonds in the hydroxyl (C—OH) and ether (C—O—C) groups. The comparison of the C1s spectra between GAC and Zr-GAC shows that the relative content of the C—C group decreases after the loading of zirconium and the O-containing groups increase on the surface of the activated carbon. XPS O1s orbital analysis is shown in Fig. 3(b). The O1s spectrum of GAC is deconvoluted into two peaks, 532.1 eV for the C—O bond and 534.8 eV for adsorbed oxygen[24-25]. For Zr-GAC, it is also fitted to two peaks, 532.1 eV and 530.5 eV, which is assigned to the Zr—OH group[24]. An increase in the relative content of C—O is observed from the comparison between GAC and Zr-GAC, which is in agreement with the result of the C1s analysis. The appearance of Z—OH indicates zirconium oxyhydroxide was formed on the surface

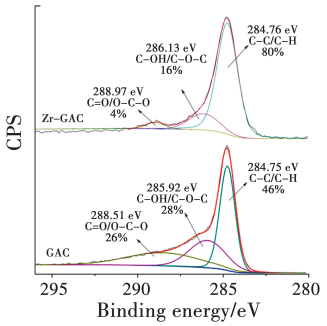

(a) C1s orbital analysis

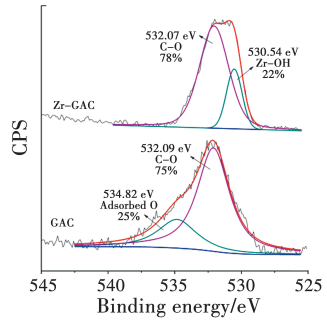

(b) O1s orbital analysis

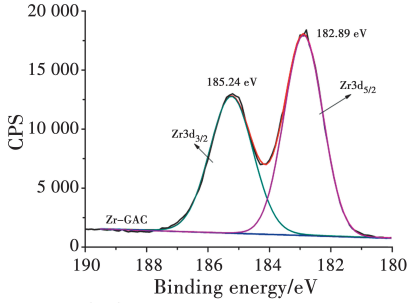

(c) Zr3d orbital for Zr-GAC

Fig. 3 XPS characterization of GAC and Zr-GAC

of Zr-GAC. XPS Zr3d orbital analysis for Zr-GAC is shown in Fig. 3(c). The Zr3d orbital includes two sub-orbital, $Zr3d_{3/2}$ at 185.3 eV and $Zr3d_{5/2}$ at 182.9 eV, which proves the presence of positive tetravalent zirconium ions[26-27].

3.4 BET surface area and pore structure

Table 2 shows the BET-N_2 specific surface area (SSA), total pore volume (TPV), and average pore diameter (APD) of GAC and Zr-GAC. The SSA of Zr-GAC is much lower than that of GAC, which may result from the fact that the loading of zirconium oxides blocked the pore structure in GAC and decreased the adsorption of N_2 in the measurement process. Both the TPV and APD of GAC increase after modification with zirconium oxides, suggesting that pores with large diameter are introduced in Zr-GAC and mesopores with diameter larger than 2 nm are the main source contributing to the specific surface area.

Table 2 BET-N_2 specific surface area (SSA), total pore volume (TPV), and average pore diameter (APD) of GAC and Zr-GAC

Adsorbent	SSA/($m^2 \cdot g^{-1}$)	TPV/($cm^3 \cdot g^{-1}$)	APD/nm
GAC	759	4.6	0.24
Zr-GAC	289.4	17.1	2.6

3.5 Effect of pH on adsorption of sulfate ions

pH plays an important role in the adsorption of ionic species in aqueous solution. The changes of sulfate adsorption on Zr-GAC along with changes in solution pH are shown in Fig. 4. The two experimental curves obtained at low and high initial sulfate concentration exhibit similar trends. The adsorption of sulfate slightly decreases with pH changing from acidic to weak base, and it drastically falls down when the solution pH exceeds approximately 10. This result indicates that the acidic condition favors the adsorption of sulfate on Zr-GAC material. To understand this pH-dependent process, the property of hydrous zirconium oxides should be taken into account. In the acidic solution, hydrous zirconium oxide is easily protonated and positively charged[19], resulting in a high chemical affinity with negatively charged sulfate ions. Previous studies showed that anionic species are mainly adsorbed on zirconium oxides via ion exchange in aqueous solution. In the present study, an increase of pH in solution after adsorption is also observed. However, the increase of the hydroxyl ion (OH^-) is not in a fixed proportion to the sulfate adsorption amount. Perhaps other anions which could form a complex compound with Zr^{4+} are involved in the sulfate adsorption process, such as chloride ions. In other words, sulfate adsorption on Zr-GAC is probably through complicated ligand exchange processes rather than a simple ion exchange process[28]. Therefore, a large number of OH^- in solution compete with sulfate ions for active adsorption sites at high pH conditions, resulting in a decrease in the adsorption capacity of sulfate.

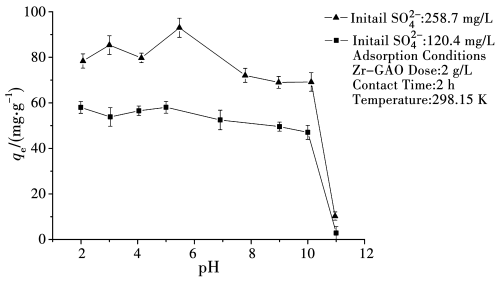

Fig. 4 Adsorption of sulfate on Zr-GAC under different solution pH

3.6 Adsorption isotherms of sulfate ions

Sulfate adsorption isotherms of GAC and Zr-GAC are presented in Fig. 5. The adsorption isotherm of Zr-GAC ascends very fast at lower sulfate concentrations. With the increase of the initial sulfate concentration, equilibrium adsorption amount, q_e, finally reaches a limiting value, implying there is a strong affinity between sulfate ions and Zr-GAC. For GAC, the adsorption of sulfate is much lower than that of Zr-GAC under the same experimental conditions, suggesting that sulfate adsorption is significantly improved by

loading zirconium oxides on activated carbon. The experimental adsorption isotherms need to be analyzed with theoretical models in order to obtain some important parameters as well as to understand the adsorption equilibrium.

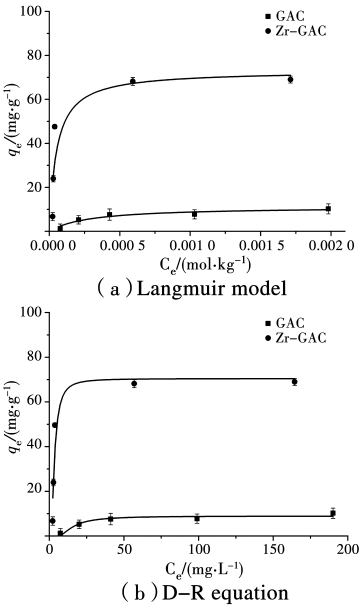

Fig. 5 Sulfate adsorption isotherms of GAC and Zr-GAC and modeling analysis

The Langmuir equation is the most widely used two-parameter model for the interpretation of adsorption equilibrium. The basic assumption of this model is a single-layer adsorption of the adsorbate on the homogeneous surface of the adsorbent[29-30]. The Langmuir equation is represented as

$$q_e = q_{max} \cdot \frac{K_L \cdot C_e}{1 + K_L \cdot C_e} \quad (2)$$

where q_e and q_{max} are respectively the equilibrium adsorption amount and the maximum adsorption amount (known as adsorption capacity corresponding to complete monolayer coverage), K_L is the Langmuir constant that represents the equilibrium constant, and C_e is the equilibrium concentration of the adsorbate in solution. In the present work, to make K_L have the meaning of standard equilibrium constants, C_e is substituted with C_e/C^θ to eliminate the effect of the concentration unit. This change gives

$$q_e = q_{max} \cdot \frac{K_L \cdot C_e/C^\theta}{1 + K_L \cdot C_e/C^\theta} \quad (3)$$

where C^θ to is equal to mol/L. From the adsorption equilibrium constant (K_L), the free energy of adsorption can be evaluated via the Gibbs equation[31], which is shown in Eq. (4).

$$\Delta G^\theta = -RT\ln(K^\theta) \quad (4)$$

where K^θ is substituted with K_L in the present work. Analysis of sulfate adsorption on GAC and Zr-GAC by the Langmuir model is shown in Fig. 5 (a), and the related parameters are summarized in Table 3. The Langmuir model gives ordinary fit to the GAC and Zr-GAC isotherms with R^2 near to 0.9. The monolayer adsorption capacity (q_m) of Zr-GAC (73.09 mg/g) for sulfate is much higher than that of GAC (11.24 mg/g). The enhancement in sulfate adsorption should be attributed to the loading of zirconium oxides on activated carbon. The free energy for sulfate adsorption on Zr-GAC is calculated as −24.48 kJ/mol, which is lower than that of GAC, suggesting a much stronger affinity between the sulfate ions and Zr-GAC surface. In addition, the accessibility of the adsorbent surface to sulfate can be estimated by calculating the maximum proportion of the BET surface area occupied by sulfate ions. Assuming that sulfate is spherical with a radius of 149 pm (S-O bond length) and in a close-packed hexagonal arrangement on the adsorbent surface[32], the area occupied per sulfate ion was calculated to be 5.77×10^{-20} m^2. Then, the maximum fraction (X_m) of the BET surface area covered by sulfate ions was estimated according to q_m that represents the limiting number of adsorption sites on the adsorbent surface. The X_m values for GAC and Zr-GAC are also shown in Table 3. Zr-GAC has a much larger X_m than that of GAC, indicating that modification with zirconium oxides significantly enhances the accessibility of the activated carbon surface to sulfate ions.

Table 3 Parameters of Langmuir and D-R equation for adsorption of sulfate

Adsorbent	Langmuir model					D-R equation			
	Q_{max}/(mg·g^{-1})	K_L	R^2	ΔG/(kJ·mol^{-1})	X_m/%	q_{DR}/(mg·g^{-1})	B	R^2	E/(kJ·mol^{-1})
GAC	11.24	3 485	0.896	−20.22	0.54	8.90	3.59×10^{-5}	0.962	0.118
Zr-GAC	73.09	19 430	0.883	−24.48	9.14	70.14	1.74×10^{-6}	0.921	0.536

These adsorption isotherms also were analyzed bythe Dubinin-Radushkevich (D-R) equation. In deriving the D-R equation for liquid-phase adsorption, the adsorption amount corresponding to any adsorbate concentration is assumed to be a Gaussian distribution of the Polanyi potential (ε)[32-34]. Thus, the D-R equation is shown as follows.

$$q_e = q_{DR}\exp(-B\varepsilon^2) \quad (5)$$

with

$$\varepsilon = RT\ln(1+1/C_e) \quad (6)$$

where q_{DR} is the maximum adsorption amount of sulfate, and B is a constant related to the characteristic adsorption energy (E_0). If the adsorbent has a heterogeneous surface and an approximation to a Langmuir isotherm is selected as the local isotherm on each homogeneous subregion, then the most probable characteristic adsorption energy is[32]

$$E_0 = (2B)^{-1/2} \quad (7)$$

Therefore, the D-R adsorption equation can be applied to estimate not only the maximum adsorption amount, but also the characteristic adsorption energy. The analysis result for sulfate adsorption on GAC and Zr-GAC are shown in Fig. 5(b), and the related parameters are presented in Table 3. The correlation coefficients (R^2) suggest that the fittings with the D-R equation are fairly good for the adsorption of both GAC and Zr-GAC. Zr-GAC has a much larger adsorption capacity (q_{DR}) than that of GAC, determined by the D-R equation. This result is similar to the result of the Langmuir model. The adsorption capacity determined by the D-R equation is a little lower than that of the Langmuir model. The characteristic adsorption energies determined by the D-R equation are also shown in Table 3. The adsorption on Zr-GAC has a higher characteristic energy than that of GAC, indicating a much stronger interaction force was formed between the sulfate ions and the active sites on the surface of Zr-GAC. This result is in agreement with the result from the Langmuir model that Zr-GAC has a higher adsorption equilibrium constant and a correspondingly higher adsorption energy. However, the characteristic adsorption energy from the D-R equation is not on the same order of magnitude as the free energy (ΔG) determined by the Langmuir model. In our opinion, the estimation of the adsorption energy by the Langmuir model is more credible because the method based on the Gibbs equation is widely accepted and the results in this work are comparable with the values in reported studies[30, 32]. Therefore, the real meaning of the parameter (E_0) in the D-R equation needs further discussion when it is applied to a solution adsorption. Perhaps an unknown conversion on E_0 should be developed to make it have a similar meaning with free energy for a specific adsorption process.

Comparison of the Zr-GAC with other sulfate adsorbents is shown in Table 4. The Zr-GAC has a relatively high adsorption capacity for sulfate ions and a good pH adaptability in contrast with most other adsorbents. The adsorption capacity of Zr-GAC is approximately two times that of zirconium oxides-loaded biochar, which was prepared for sulfate adsorption in a recent study[11]. This enhancement in adsorption capacity can be attributed to the fact that GAC has a much larger specific area as a support than biochar material, which results in a higher loading-amount of zirconium oxides. Therefore, the Zr-GAC exhibits good potential for sulfate adsorption in aqueous solution.

Table 4 Comparison of adsorption capacity of Zr-GAC with other sulfate adsorbents

Adsorbents	Adsorption capacity/(mg·g^{-1})	Solution pH	References
r-Al_2O_3	7.7	5.7	[35]
Activated carbon from coconut coir pith	4.9	4.0	[36]
ZrO_2-modified sugarcane bagasse cellulose	38.4	-	[10]
Poly(m-phenylenediamine)	108.5	1.75	[37]
Mg-Al layered double hydroxide	12.5	7	[31]
Carbon residue modified with $FeCl_3$	19.5	4	[4]
Zirconium-based MOF	56	-	[8]
Metal layered double hydroxidesfuncionalized high phoshprus ion ore waste	29～34	-	[2]
Zirconium oxides-loaded biochar	35.21	2	[11]
Zr-GAC	70.14	6.8	Present study

The symbol "-" means data are not reported.

3.7 Adsorption kinetics of sulfate ions

The changes of sulfate adsorption on Zr-GAC with contact time are shown in Fig. 6. The adsorption amount q_t increases fast within the initial 20 minutes, and then it tends to be stable, meaning adsorption equilibrium or near equilibrium is achieved. The rapid adsorption probably results from the chemical affinity between sulfate ions and zirconium oxides on the surface of the GAC, which can be considered as active adsorption sites. In addition, the sulfate adsorption is a little better at 298 K than at 283 K, suggesting high temperature may favor the adsorption.

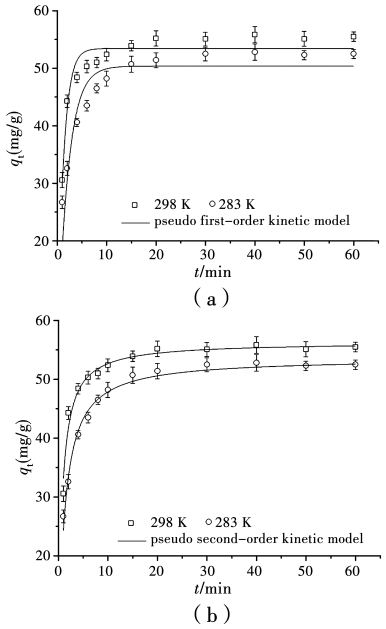

Fig. 6 Adsorption kinetics of sulfate ion on Zr-GAC

In order to describe the overall adsorption rate, kinetic data are analyzed with pseudo first- and second-order kinetic equations, which are presented in Eq. (8) and Eq. (9)[38-39], respectively.

$$\frac{dq_t}{dt} = k_{p1}(q_e - q_t) \tag{8}$$

$$\frac{dq_t}{dt} = k_{p2}(q_e - q_t)^2 \tag{9}$$

The parameters, q_e and q_t (mg/g), denote the sulfate adsorption amount at equilibrium and time t, respectively. The k_{p1} (1/min) and k_{p2} (g/(mg·min)) are the pseudo first-and second-order rate constants, respectively. The fitting results are shown in Fig. 6(a) and 6(b), and the related parameters are summarized in Table 5. The correlation coefficient (R^2) of the pseudo second-order equation is greater than that of the pseudo first-order equation, both for 298 K and for 283 K. In addition, the equilibrium adsorption amount calculated from the pseudo second-order equation agrees perfectly with the experimental value, which deviates considerably from the value determined by the pseudo first-order equation. This suggests that the adsorption of sulfate ions on Zr-GAC follows the pseudo second-order kinetic equation, which means the adsorption rate is proportional to the square of sorption driving force $(q_e - q_t)^2$. Table 5 also shows that both the equilibrium adsorption amount (q_e) and the rate

constant k_{p2} improve with the increase of the adsorption temperature from 283 K to 298 K, which confirms that the increase of temperature facilitates the adsorption of sulfate on the Zr-GAC.

Table 5 Parameters of pseudo first- and second-order kinetic models for sulfate adsorption on Zr-GAC

T/K	$q_{e,Exp}$/(mg·g^{-1})	Pseudo first-order equation			Pseudo second-order equation		
		$q_{e,Cal}$/(mg·g^{-1})	k_{p1}/(1·min^{-1})	R^2	$q_{e,Cal}$/(mg·g^{-1})	k_{p2}/(g·(mg·min)$^{-1}$)	R^2
283	52.5	50.4	0.469	0.825	53.6	0.015	0.985
298	55.3	53.4	0.809	0.880	56.3	0.025	0.968

4 Conclusion

In this work, zirconium oxides were successfully loaded on the surface of granular activated carbon to prepare an adsorbent, Zr-GAC for sulfate adsorption in aqueous solution. The SEM images show that the Zr-GAC has a porous surface with many aggregates, which are composed of zirconium oxides probed by the XRD analysis. The XPS characterization confirms the presence of zirconium and hydroxyl groups on the adsorbent surface. The BET specific surface area of activated carbon decreases after the loading of zirconium oxides, whereas the total pore volume and average pore diameter increase. Adsorption of sulfate ions on Zr-GAC is a pH-dependent process, and better adsorptions can be achieved at pH lower than 10. The adsorption isotherms were analyzed by the Langmuir and the D-R equation, and better fitting was achieved with the latter model. According to the D-R equation, the Zr-GAC has a much higher adsorption capacity (70.14 mg/g) than GAC (8.90 mg/g) in the neutral water solution. It is noticed that the D-R equation may have a problem in determining the adsorption energy for a solution adsorption, which deserves more discussion. Adsorption of sulfate on the Zr-GAC is relatively fast, and kinetic studies show that the adsorption follows the pseudo second-order kinetic equation. In addition, an increase of temperature may facilitate sulfate adsorption, to some extent.

Acknowledgements

The authors would like to acknowledge the financial support from the National Natural Science Foundation of China (No. 51408239), Natural Science Foundation of Fujian Province (No. 2016J01193), the Fundamental Research Funds for the Central Universities (No. ZQN-712) and Subsidized Project for Postgraduates' Innovative Fund in Scientific Research of Huaqiao University.

References:

[1] CAMMACK K M, WRIGHT C L, AUSTIN K J, et al. Effects of high-sulfur water and clinoptilolite on health and growth performance of steers fed forage-based diets [J]. Journal of Animal Science, 2010, 88(5): 1777-1785.

[2] PAGE M J, QUINN J E, SOLDENHOFF K H. The impact of sulfate ions on the ion exchange of rare earth elements [J]. Hydrometallurgy, 2019, 186: 12-20.

[3] DOU W X, ZHOU Z, JIANG L M, et al. Sulfate removal from wastewater using ettringite precipitation: Magnesium ion inhibition and process optimization [J]. Journal of Environmental Management, 2017, 196: 518-526.

[4] RUNTTI H, TUOMIKOSKI S, KANGAS T, et al. Sulphate removal from water by carbon residue from biomass gasification: effect of chemical modification methods on sulphate removal efficiency [J]. BioResources, 2016, 11(2): 3136-3152.

[5] AMARAL FILHO J, AZEVEDO A, ETCHEPARE R, et al. Removal of sulfate ions by dissolved air flotation (DAF) following precipitation and flocculation [J]. International Journal of Mineral Processing, 2016, 149: 1-8.

[6] SADEGHALVAD B, AZADMEHR A, HEZARKHANI A. Sulfate decontamination from groundwater by metal layered double hydroxides functionalized high phosphorus iron ore waste as a new green adsorbent:

Experimental and modeling [J]. Ecological Engineering, 2017, 106: 219-230.

[7] SOLGI M, TABIL L G, WILSON L D. Modified biopolymer adsorbents for column treatment of sulfate species in saline aquifers [J]. Materials, 2020, 13(10): 2408.

[8] HOWARTH A J, WANG T C, AL-JUAID S S, et al. Efficient extraction of sulfate from water using a Zr-metal-organic framework [J]. Dalton Transactions, 2016, 45(1): 93-97.

[9] SAIKI K, YOSHIDA N, SILVER M M. New desulfation system for chlor-alkali plant [J]. Special Publication-Royal Society of Chemistry, 1995, 164: 82-82.

[10] MULINARI D R, DA SILVA M L C P. Adsorption of sulphate ions by modification of sugarcane bagasse cellulose [J]. Carbohydrate Polymers, 2008, 74(3): 617-620.

[11] AO H T, CAO W, HONG Y X, et al. Adsorption of sulfate ion from water by zirconium oxide-modified biochar derived from pomelo peel [J]. Science of The Total Environment, 2020, 708: 135092.

[12] SCHMIDT G T, VLASOVA N, ZUZAAN D, et al. Adsorption mechanism of arsenate byzirconyl-functionalized activated carbon [J]. Journal of Colloid and Interface Science, 2008, 317(1): 228-234.

[13] HASHITANI H, OKUMURA M, FUJINAGA K. Effective preconcentration method for fluoride ions from dilute aqueous solution by activated carbon loaded with zirconium [J]. Fresenius'Zeitschrift Für Analytische Chemie, 1985, 320(8): 774.

[14] HASHITANI H, OKUMURA M, FUJINAGA K. Preconcentration method for phosphate in water using activated carbon loaded with zirconium [J]. Fresenius'Zeitschrift Für Analytische Chemie, 1987, 326(6): 540-542.

[15] TANSEL B, NAGARAJAN P. SEM study of phenolphthalein adsorption on granular activated carbon [J]. Advances in Environmental Research, 2004, 8(3/4): 411-415.

[16] HESCHEL W, KLOSE E. On the suitability of agricultural by-products for the manufacture of granular activated carbon [J]. Fuel, 1995, 74(12): 1786-1791.

[17] PRAHAS D, KARTIKA Y, INDRASWATI N, et al. Activated carbon from jackfruit peel waste by H_3PO_4 chemical activation: Pore structure and surface chemistry characterization [J]. Chemical Engineering Journal, 2008, 140(1/2/3): 32-42.

[18] AZARGOHAR R, DALAI A K. Biochar as a precursor of activated carbon [J]. Applied Biochemistry and Biotechnology, 2006, 129-132: 762-773.

[19] SUZUKI T M, BOMANI J O, MATSUNAGA H, et al. Preparation of porous resin loaded with crystalline hydrous zirconium oxide and its application to the removal of arsenic [J]. Reactive and Functional Polymers, 2000, 43(1/2): 165-172.

[20] DAMYANOVA S, PAWELEC B, ARISHTIROVA K, et al. Study of the surface and redox properties of ceria-zirconia oxides [J]. Applied Catalysis A: General, 2008, 337(1): 86-96.

[21] GOWRI S, RAJIV GANDHI R, SUNDRARAJAN M. Structural, optical, antibacterial and antifungal properties of zirconia nanoparticles by biobased protocol [J]. Journal of Materials Science & Technology, 2014, 30(8): 782-790.

[22] CAO W, WANG Z Q, ZENG Q L, et al. ^{13}C NMR and XPS characterization of anion adsorbent with quaternary ammonium groups prepared from rice straw, corn stalk and sugarcane bagasse [J]. Applied Surface Science, 2016, 389: 404-410.

[23] ZAFAR A, SCHJØDT-THOMSEN J, SODHI R, et al. X-ray photoelectron spectroscopy and time-of-flight secondary ion mass spectrometry characterization of aging effects on the mineral fibers treated with aminopropylsilane and quaternary ammonium compounds [J]. Surface and Interface Analysis, 2012, 44(7): 811-818

[24] HE J G, LI Y, XUE X X, et al. Separation of fluorine/cerium from fluorine-bearing rare earth sulfate solution by selective adsorption using hydrous zirconium oxide [J]. RSC Advances, 2016, 6(49): 43814-43822.

[25] PENG Y, LIU R, CAO J Z. Characterization of surface chemistry and crystallization behavior of polypropylene composites reinforced with wood flour, cellulose, and lignin during accelerated weathering [J]. Applied Surface Science, 2015, 332: 253-259.

[26] WANG X Z, PAN S L, ZHANG M, et al. Modified hydrous zirconium oxide/PAN nanofibers for efficient defluoridation from groundwater [J]. Science of The

Total Environment, 2019, 685: 401-409.

[27] YU Z C, XU C H, YUAN K K, et al. Characterization and adsorption mechanism of ZrO_2 mesoporous fibers for health-hazardous fluoride removal [J]. Journal of Hazardous Materials, 2018, 346: 82-92.

[28] RODRIGUES L A, MULINARI D R, SILVA M L C P. Adsorption of sulfate ions in $ZrO_2 . nH_2O$ prepared by conventional precipitation and homogeneous solution methods [J]. Cerâmica, 2009, 55(333): 40-45.

[29] ZHENG L C, DANG Z, YI X Y, et al. Equilibrium and kinetic studies of adsorption of Cd (II) from aqueous solution using modified corn stalk [J]. Journal of Hazardous Materials, 2010, 176(1/2/3): 650-656.

[30] DRAGAN E S, HUMELNICU D, DINU M V, et al. Kinetics, equilibrium modeling, and thermodynamics on removal of Cr(VI) ions from aqueous solution using novel composites with strong base anion exchanger microspheres embedded into chitosan/poly (vinyl amine) cryogels [J]. Chemical Engineering Journal, 2017, 330: 675-691.

[31] HALAJNIA A, OUSTAN S, NAJAFI N, et al. Adsorption-desorption characteristics of nitrate, phosphate and sulfate on Mg-Al layered double hydroxide [J]. Applied Clay Science, 2013, 80/81: 305-312.

[32] HSIEH C T, TENG H. Langmuir and Dubinin-Radushkevich analyses on equilibrium adsorption of activated carbon fabrics in aqueous solutions [J]. Journal of Chemical Technology & Biotechnology, 2000, 75(11)1066-1072

[33] CATURLA F, MARTÍN-MARTÍNEZ J M, MOLINA-SABIO M, et al. Adsorption of substituted phenols on activated carbon [J]. Journal of Colloid and Interface Science, 1988, 124(2): 528-534.

[34] HOBSON J P. Physical adsorption isotherms extending from ultrahigh vacuum to vapor pressure [J]. The Journal of Physical Chemistry, 1969, 73 (8): 2720-2727.

[35] WU C H, KUO C Y, LIN C F, et al. Modeling competitive adsorption of molybdate, sulfate, selenate, and selenite using a Freundlich-type multi-component isotherm [J]. Chemosphere, 2002, 47(3): 283-292.

[36] NAMASIVAYAM C, SANGEETHA D. Application of coconut coir pith for the removal of sulfate and other anions from water [J]. Desalination, 2008, 219(1/2/3): 1-13.

[37] SANG P L, WANG Y Y, ZHANG L Y, et al. Effective adsorption of sulfate ions with poly (m-phenylenediamine) in aqueous solution and its adsorption mechanism [J]. Transactions of Nonferrous Metals Society of China, 2013, 23(1): 243-252.

[38] QIU H, LV L, PAN B C, et al. Critical review in adsorption kinetic models [J]. Journal of Zhejiang University-Science A, 2009, 10(5): 716-724.

[39] HO Y S, MCKAY G. Pseudo-second order model for sorption processes [J]. Process Biochemistry, 1999, 34(5): 451-465.

(编辑 胡英奎)